



## Measured and modeled CO and NO<sub>y</sub> in DISCOVER-AQ: An evaluation of emissions and chemistry over the eastern US



Daniel C. Anderson<sup>a,\*</sup>, Christopher P. Loughner<sup>b,c</sup>, Glenn Diskin<sup>d</sup>, Andrew Weinheimer<sup>e</sup>, Timothy P. Canty<sup>a</sup>, Ross J. Salawitch<sup>a,b</sup>, Helen M. Worden<sup>e</sup>, Alan Fried<sup>f</sup>, Tomas Mikoviny<sup>g,1</sup>, Armin Wisthaler<sup>h,1</sup>, Russell R. Dickerson<sup>a</sup>

<sup>a</sup> Department of Atmospheric and Oceanic Sciences, University of Maryland, College Park, MD 20742, USA

<sup>b</sup> Earth System Science Interdisciplinary Center, University of Maryland, College Park, MD 20740, USA

<sup>c</sup> NASA Goddard Space Flight Center, Greenbelt, MD 20771, USA

<sup>d</sup> NASA Langley Research Center, Hampton, VA 23681, USA

<sup>e</sup> National Center for Atmospheric Research, Boulder, CO 80305, USA

<sup>f</sup> Institute of Arctic and Alpine Research, University of Colorado, Boulder, CO 80303, USA

<sup>g</sup> Oak Ridge Associated Universities, Oak Ridge, TN 37830, USA

<sup>h</sup> Institut für Ionenphysik und Angewandte Physik, Universität Innsbruck, Innsbruck, Austria

### HIGHLIGHTS

- The observed molar CO/NO<sub>x</sub> emissions ratio in Washington/Baltimore is 11.2 ± 1.2.
- The NEI overestimates mobile NO<sub>x</sub> emissions by between 51 and 70%.
- *In situ* & MOPITT observed & CMAQ modeled CO show excellent agreement.
- CMAQ's overestimate of NO<sub>y</sub> results from errors in both chemistry and emissions.

### ARTICLE INFO

#### Article history:

Received 13 March 2014

Received in revised form

30 June 2014

Accepted 2 July 2014

Available online 3 July 2014

#### Keywords:

Air quality

National Emissions Inventory

CO

NO<sub>x</sub>

On-road emissions

CMAQ

### ABSTRACT

Data collected during the 2011 DISCOVER-AQ field campaign in the Baltimore Washington region were used to evaluate CO and NO<sub>x</sub> emissions in the National Emissions Inventory (NEI). The average emissions ratio for the region was seen to be 11.2 ± 1.2 mol CO/mol NO<sub>x</sub>, 21% higher than that predicted by the NEI. Comparisons between *in situ* and remote observations and CMAQ model output show agreement in CO emissions of 15 ± 11% while NO<sub>x</sub> emissions are overestimated by 51–70% in Maryland. Satellite observations of CO by MOPITT show agreement with the Community Multiscale Air Quality (CMAQ) model within 3% over most of the eastern United States. CMAQ NO<sub>y</sub> mixing ratios were a factor of two higher than observations and result from a combination of errors in emissions and PAN and alkyl nitrate chemistry, as shown by comparison of three CMAQ model runs. Point source NO<sub>x</sub> emissions are monitored and agree with modeled emissions within 1% on a monthly basis. Because of this accuracy and the NEI assertion that approximately 3/4 of emissions in the Baltimore Washington region are from mobile sources, the MOVES model's treatment of emissions from aging vehicles should be investigated; the NEI overestimate of NO<sub>x</sub> emissions could indicate that engines produce less NO<sub>x</sub> and catalytic converters degrade more slowly than assumed by MOVES2010. The recently released 2011 NEI has an even lower CO/NO<sub>x</sub> emissions ratio than the projection used in this study; it overestimates NO<sub>x</sub> emissions by an even larger margin. The implications of these findings for US air quality policy are that NO<sub>x</sub> concentrations near areas of heavy traffic are overestimated and ozone production rates in these locations are slower than models indicate. Results also indicate that ambient ozone concentrations will respond more efficiently to NO<sub>x</sub> emissions controls but additional sources may need to be targeted for reductions.

© 2014 Elsevier Ltd. All rights reserved.

\* Corresponding author.

E-mail address: [danderson@atmos.umd.edu](mailto:danderson@atmos.umd.edu) (D.C. Anderson).

<sup>1</sup> Now at: Department of Chemistry, University of Oslo, Oslo, Norway.

## 1. Introduction

Both  $\text{NO}_x$  ( $\text{NO} + \text{NO}_2$ ) and CO adversely affect human health and are  $\text{O}_3$  precursors, a secondary air pollutant that can cause respiratory ailments in vulnerable populations (Bell et al., 2006; US EPA, 2008; 2010). Enactment of the Clean Air Act (CAA) has significantly reduced CO and  $\text{NO}_x$  concentrations in the United States (US). Maximum ambient CO concentrations in urban areas decreased by a factor of three between 1977 and 2000 while  $\text{NO}_x$  concentrations have decreased by a factor of two over the same period, putting both species well below the National Ambient Air Quality Standards (NAAQS) set by the Environmental Protection Agency (EPA) (He et al., 2013; Parrish, 2006).  $\text{O}_3$  concentrations have decreased comparatively little, with multiple sites across the country exceeding NAAQS limits (Cooper et al., 2012; Fiore et al., 1998). This is particularly true in the Baltimore/Washington Region (BWR) which has significant surface  $\text{O}_3$  throughout, especially over the Chesapeake Bay (Goldberg et al., 2014).

The reduction in ambient CO and  $\text{NO}_x$  concentrations is reflected in estimates of changes in emissions (Bishop et al., 2012). National, on-road  $\text{NO}_x$  emissions decreased by ~65% between 1990 and 2010 (McDonald et al., 2012). Different regulatory strategies for diesel and light duty vehicles have increased the ratio of diesel to light duty  $\text{NO}_x$  emissions by a factor of two between 1997 and 2006, with diesel emissions now accounting for ~75% of mobile  $\text{NO}_x$  emissions (both on- and off-road) (Ban-Weiss et al., 2008; Dallmann and Harley, 2010). For light duty vehicles, emissions from about 1% of the fleet are responsible for almost 33% of CO and 16% of  $\text{NO}_x$  emissions (Bishop et al., 2012). These significant changes in emissions and sources must be accurately reflected in inventories, such as the National Emissions Inventory (NEI), to allow for proper estimation of  $\text{NO}_x$  and CO concentrations used in air quality models and for the development of policies to reduce ambient  $\text{O}_3$ .

The EPA produces the NEI every three years, estimating annual, county-level emissions of criteria air pollutants from On-Road, Off-Road, Point, and Area sources. States can use these emissions to develop State Implementation Plans (SIPs) as part of their obligation to reduce ambient pollution under the CAA. The 2011 NEI estimates nationwide emissions of  $7.6 \times 10^7$  ( $2.5 \times 10^{12}$ ) and  $1.45 \times 10^7$  ( $2.9 \times 10^{11}$ ) short tons (moles) of CO and  $\text{NO}_x$  respectively, assuming  $\text{NO}_x$  is emitted as  $\text{NO}_2$ . According to the NEI, nationally, mobile sources (both on- and off-road) account for 55% of CO and 62% of  $\text{NO}_x$  emissions; electricity generation accounts for 1% of CO and 14% of  $\text{NO}_x$ . The relative importance of mobile CO and  $\text{NO}_x$  emissions is even larger in Maryland, accounting for 86% and 73% of total emissions respectively.

Multiple attempts to evaluate the NEI's accuracy over different spatial scales have provided conflicting results for CO and  $\text{NO}_x$ . In a tunnel study in Van Nuys California, Fujita et al. (2012) found that the Motor Vehicle Emissions Simulator (MOVES2010) model overestimates  $\text{NO}_x$  and CO on-road emissions factors by 38–50% and 12–41% respectively. Brioude et al. (2013), using an inverse modeling approach in the Los Angeles (LA) basin, determined that NEI estimates of emissions were high for both species, CO by 37–43% and  $\text{NO}_x$  by 27–32%. Also in LA, Pollack et al. (2013) found that the observed  $\text{NO}_x/\text{CO}$  ratio was approximately half the value estimated by the California Air Resources Board emissions inventory, often regarded as more accurate than the NEI. On the national scale, Parrish (2006) concluded that the NEI overestimated CO emissions by ~100%, while  $\text{NO}_x$  emissions were accurate. Comparing measured  $\text{NO}_y$  values from Houston to output from the Community Multiscale Air Quality (CMAQ) model, Yu et al. (2012) found that modeled values of  $\text{NO}_y$  (approximately the sum of  $\text{NO}$ ,  $\text{NO}_2$ , alkyl nitrates, PANs, and  $\text{HNO}_3$ ) are a factor of two too high and conclude that NEI  $\text{NO}_x$  emissions must likewise be too high.

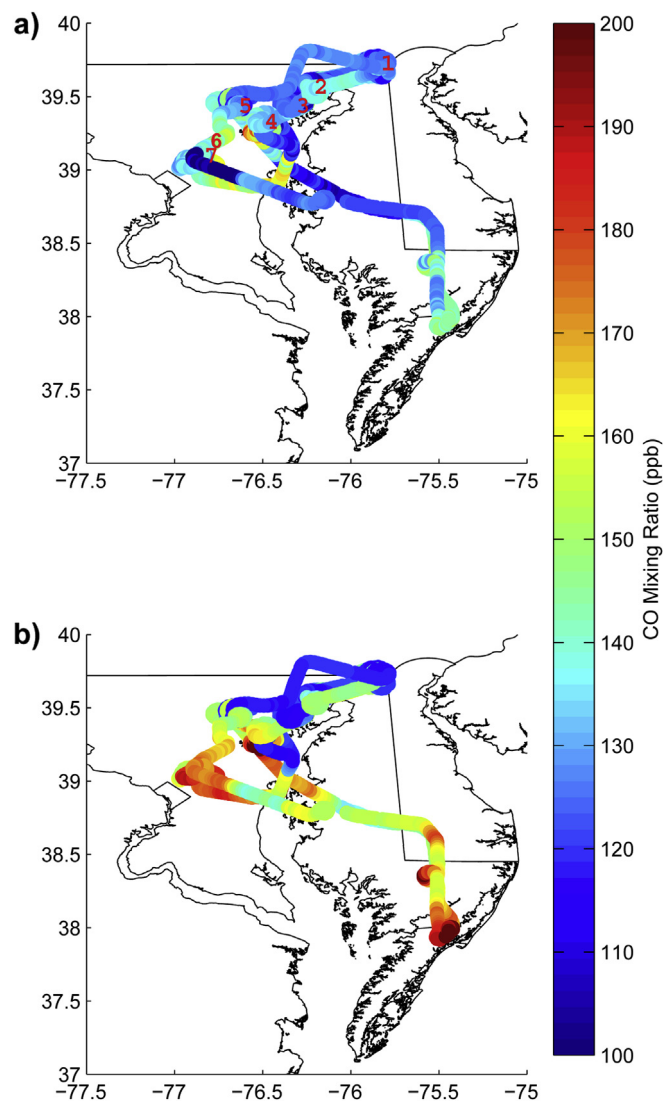


**Fig. 1.** CO along the flight track (1 July 2011). a) Observed b) Modeled. Spiral and transect locations are marked in a). 1. Fairhill 2. Aldino 3. Edgewood 4. Essex 5. Padonia 6. I-95 7. Beltsville.

In the BWR, Castellanos et al. (2011) found, from comparing observations in the RAMMPP campaign to CMAQ model output, that NEI CO emissions were correct or slightly underestimated while  $\text{NO}_x$  emissions from mobile sources were likely overestimated. There is little agreement among these studies on the NEI's accuracy, for either CO or  $\text{NO}_x$ , showing both under- and overestimation for both species.

This study attempts to evaluate the NEI for the BWR using extensive *in situ* observations from the Deriving Information on Surface conditions from Column and Vertically Resolved Observations Relevant to Air Quality (DISCOVER-AQ) field campaign. We calculate emissions ratios of CO/ $\text{NO}_x$  from these observations and compare measured concentrations to those modeled by CMAQ to evaluate emissions estimates.

## 2. Methodology

### 2.1. DISCOVER-AQ

Part 1 of DISCOVER-AQ was conducted in the BWR during July 2011. One of the mission's primary goals was to increase

understanding of severe O<sub>3</sub> episodes in the US Mid-Atlantic region. The NASA P3-B measured trace gas composition – including CO, NO, NO<sub>2</sub>, O<sub>3</sub>, HNO<sub>3</sub>, the sum of PAN and PAN-like compounds ( $\Sigma$ PAN), the sum of alkyl nitrates ( $\Sigma$ AN), and total NO<sub>y</sub> – aerosol properties, and meteorological variables. Vertical profiles for all species were obtained over six locations – Beltsville, Padonia, Fairhill, Aldino, Edgewood, and Essex – in the BWR from approximately 0.3 to 5 km above ground level. Locations coincided with ground monitors of surface pollution and provided a range of urbanization and pollution. Flights were conducted over 14 days with the flight path shown in Fig. 1, allowing for approximately three spirals at each site per day, for a total of 242. 43 horizontal transects were flown at approximately constant altitude over a segment of the I-95 interstate between Beltsville and Baltimore. All flights were during daylight hours and on days without rain. Flight days were selected to provide a mixture of lightly and heavily polluted air masses.

CO was measured using the NASA DACOM diode laser spectrometer (Sachse et al., 1987). Measurement uncertainty is 2%. CO and all other trace gases in this study were sampled at 1 Hz, unless otherwise noted and then averaged over 15 s to reduce noise and uncertainty. Total NO<sub>y</sub>, NO, NO<sub>2</sub>, and O<sub>3</sub> were measured with a 4-channel chemiluminescence instrument with an uncertainty of 20% (Ridley and Grahek, 1990). A thermal decomposition laser induced fluorescence instrument (TD-LIF) measured NO<sub>y</sub> constituents, including  $\Sigma$ PAN, HNO<sub>3</sub>, and  $\Sigma$ AN (Farmer et al., 2006). Individual species were measured at 1 Hz, but instrumental design precluded simultaneous measurement of species. Directly measured NO<sub>y</sub> and NO<sub>y</sub> calculated from the summing of constituents agree within 15% over the entire campaign.

Other measured trace gases include formaldehyde and isoprene. Formaldehyde was measured by difference frequency generation absorption spectroscopy, with a detection limit of 94 pptv and a  $1\sigma$  uncertainty of ~4% (Lancaster et al., 2000). Isoprene was measured with Proton Transfer Reaction Mass Spectrometry (P3B) and a Perkin-Elmer Gas Chromatograph – Flame Ionization Detector automated VOC analyzer (surface observations at Essex) (Lindinger et al., 1998).

## 2.2. Model setup

CMAQ model version 5.0 was run, driven offline by meteorological fields from the Weather and Research Forecasting (WRF) model 3.3, to simulate concentrations of CO and NO<sub>y</sub> over the experimental domain for July 2011 and to provide a basis of comparison between the NEI and observed emissions ratios. A complete model setup can be found in Loughner et al. (2014).

WRF was run at resolutions of 36, 12, 4, and 1.33 km in the horizontal with 34 vertical levels, ranging from 1000 to 100 hPa. The atmosphere's lowest 2 km contains 16 layers to capture variations in the planetary boundary layer (PBL) accurately. The North American Regional Reanalysis was used for initial and boundary conditions.

Anthropogenic emissions input into CMAQ were from the 2005 NEI projected to 2011, including emissions changes due to growth and emissions controls to be implemented by 2012 (US EPA, 2011). The CO/NO<sub>x</sub> emissions ratio over the state of Maryland between the recently released 2011 NEI and the projection in this study agree within 20%, with values of 7.5 and 9 mol/moles respectively, indicating that this analysis is realistic and can provide insight into the 2011 NEI. Mobile emissions from on-road vehicles were calculated with MOVES2010 (US EPA, 2012). See US EPA (2011) and the Supplementary materials for a more in-depth description of the MOVES2010 setup.

## 2.3. Calculation of emissions ratios

To calculate the emissions ratio of CO to NO<sub>x</sub> from the *in situ* observations, CO and NO<sub>y</sub> concentrations from the PBL for each spiral/transect were regressed against one another using an orthogonal linear regression, assuming uncertainties in both constituents (Crutzen et al., 1979). Because of diurnal variation in PBL depth and a lack of a clearly defined mixed layer in many spirals, a PBL depth of 1.5 and 0.7 km was assumed for all spirals after and before noon local time, respectively. The resulting slope yields the change in CO with respect to NO<sub>y</sub>. Assuming no *in situ* production or loss of either compound, this slope is the emissions ratio (ER) of CO to NO<sub>x</sub>, or  $ER = \Delta(\text{CO})/\Delta(\text{NO}_y)$ , where deltas represent the increase over background concentrations. NO<sub>y</sub> was used to estimate NO<sub>x</sub> emissions because air parcels were not measured at the emission location. Substantial conversion of NO<sub>x</sub> to NO<sub>y</sub> occurs between emission and observation, while the comparatively long NO<sub>y</sub> lifetime reduces the likelihood of NO<sub>y</sub> species loss. The implications of lifetime and the assumption of no *in situ* production or loss are discussed later.

## 3. Results

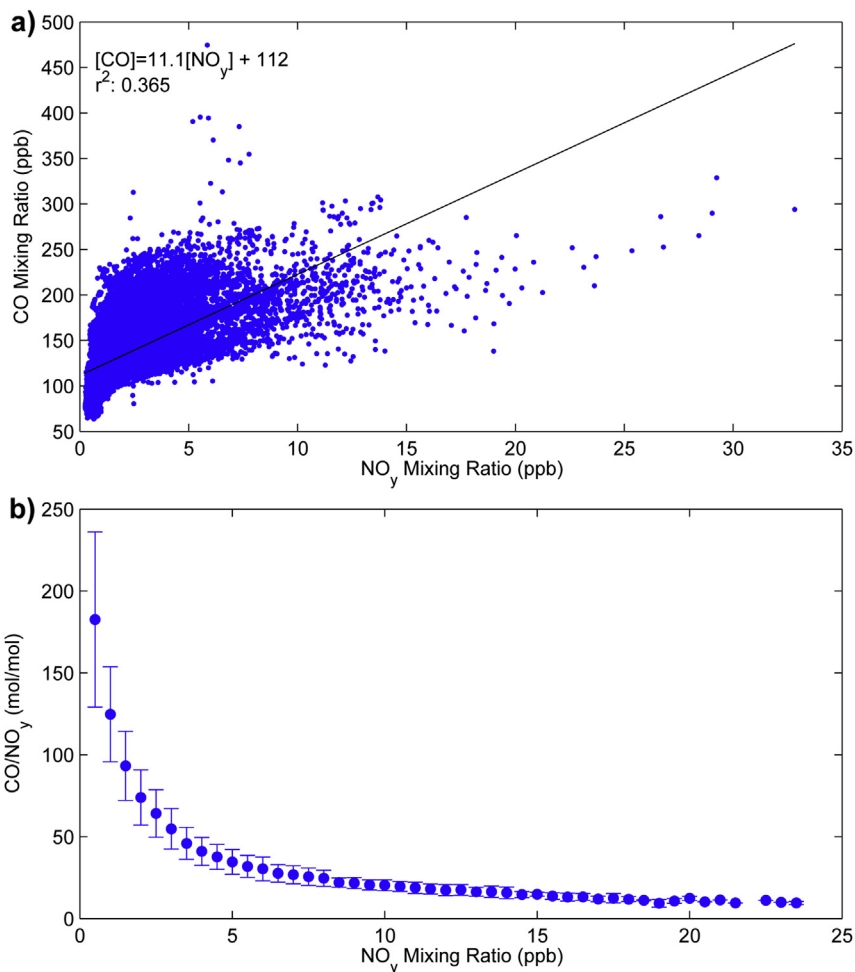
### 3.1. Measured emissions ratios

A regression of all measured CO against NO<sub>y</sub> (Fig. 2a) shows low linear correlation ( $r^2 = 0.36$ ). This likely results from the spatio-temporal variability in sampled NO<sub>x</sub> emissions. Parcels sampled later in the day or away from major sources are more likely to have NO<sub>x</sub> converted to NO<sub>y</sub> followed by deposition. Fig. 2b demonstrates this aging effect clearly. At low NO<sub>y</sub> concentrations, CO/NO<sub>y</sub> is high and almost exponentially increasing, indicating significant NO<sub>y</sub> loss. The majority of measurements lie in this regime. As the NO<sub>y</sub> concentration increases, however, CO/NO<sub>y</sub> decreases and asymptotically approaches a CO/NO<sub>y</sub> ratio of 10.5. Analysis of individual spirals and transects provide a more accurate estimate of this ratio.

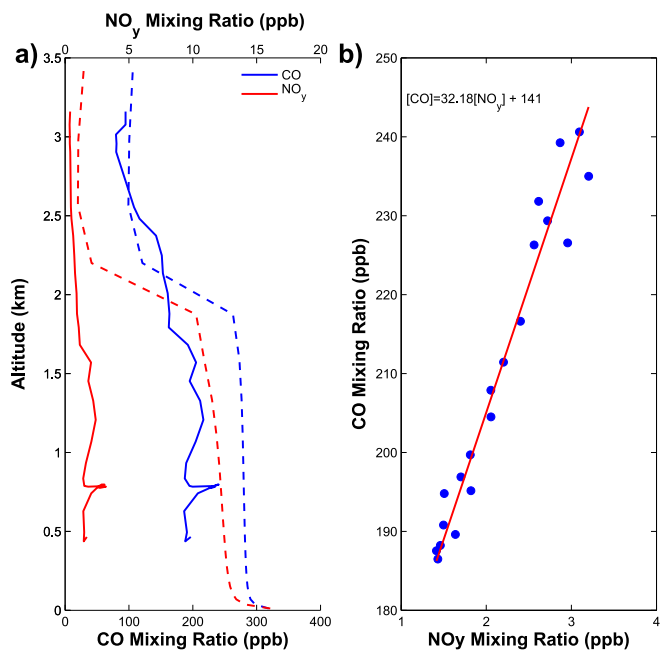
Vertical CO and NO<sub>y</sub> profiles for a sample spiral over Padonia, MD on 11 July 2011 between 16:30 and 16:50 Eastern Daylight Time (EDT) are shown in Fig. 3a. The two profiles show excellent correlation below 1.5 km, the assumed PBL height. Sharp changes in one species, indicative of different air parcels, are closely mirrored in the other, providing the degrees of freedom necessary for a regression analysis. The two species, plotted against one another in Fig. 3b, show a highly linear relationship for concentrations in the PBL. A linear relationship with a statistical significance of  $p < 0.05$  is found for 175 of the 287 spirals and transects, with a geometric average of  $11.2 \pm 1.19$  mol CO/mol NO<sub>x</sub>. Total uncertainty is the mean of the fit uncertainty of each regression added in quadrature with the mean of the standard errors for each site. Geometric means reflect the dominant mode of the emissions ratio distribution, which is more lognormal than Gaussian.

Fig. 4 shows the distribution, by location, of observed ratios for all spirals and transects with  $p < 0.05$ . Ratios varied significantly among the sites, with values at Edgewood,  $8.36 \pm 0.95$ , almost a factor of 2 lower than those at Aldino,  $15.3 \pm 1.6$ , the site with the highest mean ratio. Edgewood's proximity to the Chesapeake Bay allows for greater influence from marine emissions, which tend to emit high NO<sub>x</sub> and low CO (Williams et al., 2009). The bay breeze, a feature common to Edgewood in this study, could contribute to the low observed CO/NO<sub>x</sub> ratios, as the meteorology could allow for the accumulation or removal of pollutants, altering the observed emissions ratio.

Fig. 4 also shows the average CO/NO<sub>x</sub> emissions ratio from SMOKE by location. Values were calculated along 24-h backtrajectories (see Supplementary materials) for all measured



**Fig. 2.** a) Regression of all measured CO and NO<sub>y</sub> mixing ratios for the entire campaign. Black line is the line of best fit. b) Data from a) plotted as the ratio of CO/NO<sub>y</sub> vs NO<sub>y</sub> mixing ratio. Data are separated into 0.5 ppbv bins. Mean values are shown with error bars of  $\pm 1\sigma$ .



**Fig. 3.** a) Sample vertical profiles of CO and NO<sub>y</sub> over Padonia, MD (11 July 2011, 16:30–16:50 EDT). Solid lines are observations; dashed lines are from the 1.33 km resolution CMAQ run. b) Regression of CO and NO<sub>y</sub> in the PBL (0–1.5 km).

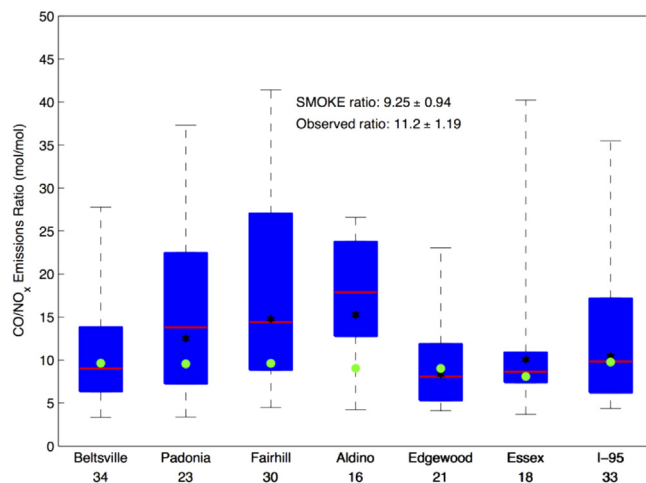


**Fig. 4.** Distribution of observed CO/NO<sub>x</sub> emissions ratios for each spiral/transect location. Red line is the median, star is the average, box edges are the 25th and 75th percentiles, and whiskers are the 5 and 95th percentiles. All other box-and-whisker plots have the same configuration. Circles show the average emissions ratio from SMOKE along 24-h backtrajectories. Numbers under the location names are the number of profiles/transects observed with correlations having a  $p < 0.05$ . (For interpretation of the references to color in this figure legend, the reader is referred to the web version of this article.)

spirals with observed correlation between CO and NO<sub>y</sub>. The NEI agrees within 10% with CO/NO<sub>y</sub> observations at Edgewood, Beltsville, and I-95, while it underestimates the ratio at the other sites by up to a factor of 1.7. Evaluation of the CO/NO<sub>x</sub> emissions ratios by linear regression of the vertical CMAQ concentration profiles is not possible. Profiles of CO and NO<sub>y</sub> at multiple CMAQ resolutions are essentially constant with height in the PBL (see Fig. 3), resulting in only one degree of freedom and no statistically significant results.

Each site exhibited significant variation in measured CO/NO<sub>y</sub> ratios, spanning an order of magnitude at some locations. Fig. 5 shows substantial diurnal variation, with the lowest average CO/NO<sub>y</sub> ratios in the morning and a general increasing tendency as the day progresses. Morning (times before noon EDT) CO/NO<sub>y</sub> ratios average  $7.93 \pm 1.07$  while afternoon values are about  $13.8 \pm 1.07$ , a 74% increase. This pattern holds true at each location, as shown in Table 1, with Edgewood significantly lower in the morning than the other sites. Afternoon values are most likely a better indicator of the actual CO/NO<sub>x</sub> emissions ratio because the PBL is more thoroughly mixed during this time. *In situ* CO production from biogenic volatile organic compounds (VOCs) oxidation also contributes to this phenomenon. Isoprene emissions peak in the early afternoon with increasing temperatures and can lead to substantial CO production (Hudman et al., 2008). Further discussion of CO production from biogenic emissions is included in the next section.

Fig. 4 also shows good agreement between CO/NO<sub>x</sub> emissions ratios in the NEI and on I-95. I-95 has a different mixture of vehicle types than the other locations, which are dominated heavily by local traffic. While an hourly breakdown of heavy-versus light-duty vehicles is not available for the portion of I-95 observed in this study, daily averages show that heavy-duty vehicles comprise approximately 10% of the traffic on I-95, although in some locations it is as high as 30%, compared to only 5% in city centers [Maryland Department of Transportation]. These measurements most likely underestimate the total fraction of heavy-duty vehicles on I-95, however, as most traffic counters are located at interstate on- and off-ramps and therefore will not include all trucks on the interstate itself. The value presented here should be viewed as a lower bound. Because diesel engines tend to emit more NO<sub>x</sub> and less CO than light duty vehicles, a larger fraction of diesel engines on I-95 as compared to the other locations in this study could explain the agreement.

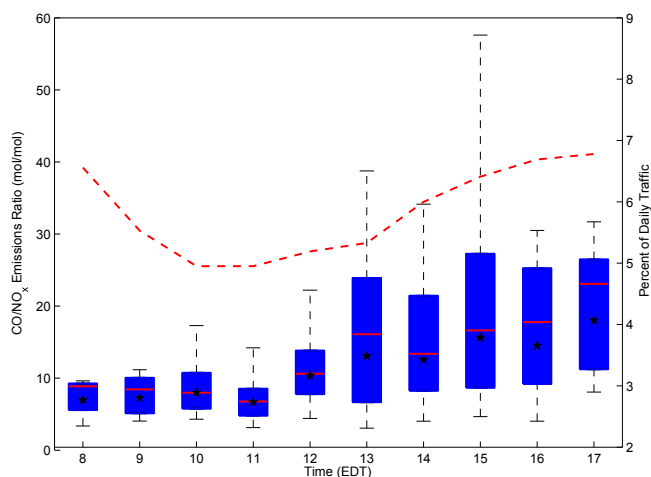


Fig. 5. The distribution of emissions ratios by time of day. Black stars are the average value for each hour. Fraction of Maryland on-highway traffic, by hour, is shown with the dotted red line. (For interpretation of the references to color in this figure legend, the reader is referred to the web version of this article.)

Table 1

Observed CO/NO<sub>y</sub> ratios by location and time. Morning and afternoon are defined as before and after 12 EDT, respectively.

Location	Latitude (°N)	Longitude (°W)	Overall	Morning	Afternoon
Fairhill	39.726	75.835	$14.8 \pm 1.43$	$8.14 \pm 1.27$	$19.9 \pm 1.44$
Aldino	39.567	76.212	$15.3 \pm 1.60$	$12.2 \pm 2.59$	$16.4 \pm 2.63$
Edgewood	39.442	76.315	$8.36 \pm 1.00$	$6.71 \pm 1.01$	$9.57 \pm 1.11$
Essex	39.333	76.494	$10.1 \pm 1.54$	$7.12 \pm 1.30$	$11.5 \pm 1.52$
Padonia	39.436	76.635	$12.5 \pm 1.64$	$8.37 \pm 1.86$	$15.5 \pm 1.94$
I-95	39.202	76.796	$10.4 \pm 0.95$	$7.98 \pm 0.77$	$13.8 \pm 0.99$
Beltsville	39.055	76.832	$9.67 \pm 1.08$	$7.54 \pm 1.02$	$11.3 \pm 1.03$
Overall	N/A	N/A	$11.2 \pm 1.19$	$7.93 \pm 1.07$	$13.8 \pm 1.07$

### 3.2. Uncertainties in the observed emissions ratio

With CO's lifetime of ~1 month, CO losses should not have any measurable effect on the observed CO/NO<sub>x</sub> ratio (Seinfeld and Pandis, 2006). Isoprene, the dominant VOC in the BWR, oxidizes to produce CO, however (Morales, 1998). Fig. 6a shows the isoprene profile over Essex for July 2011 as measured from the P3B and at the surface. Isoprene mixing ratio decreases quickly with height, dropping by greater than a factor of four from the surface to 1 km, showing isoprene's reactivity.

The relationship between formaldehyde and the CO/NO<sub>x</sub> ratio also demonstrates the effect of VOC chemistry on CO. Isoprene and other VOCs strongly promote formaldehyde formation at low altitudes in the BWR. High formaldehyde mixing ratios indicate a highly oxidative environment in which *in situ* CO formation is more likely. This effect is shown in Fig. 6b. While CO/NO<sub>x</sub> ratios vary widely at all formaldehyde mixing ratios, median CO/NO<sub>x</sub> ratios clearly increase with increasing formaldehyde concentrations, demonstrating VOC's observable effect on CO concentrations.

To calculate an upper bound on CO production from isoprene, it was assumed that the reaction of OH with isoprene would produce only CO. At the surface, isoprene-produced CO can account for as much as 45% of total CO, but because of the quick e-folding lifetime, this percentage quickly becomes negligible with increasing height, dropping to less than 1% by 0.5 km. For the total PBL column, ~6% of CO could be attributed to production from isoprene degradation.

In contrast, substantial new NO<sub>y</sub> compounds are not produced naturally, except by lightning. Because observations were made in the PBL on days without deep convection, contributions from lightning NO<sub>x</sub> are minimized. NO<sub>y</sub>, which is removed by wet and dry deposition as well as by conversion to aerosols, has an atmospheric lifetime substantially shorter than that of CO. Gaseous NO<sub>y</sub> can be removed by both dry and wet deposition as well as conversion to aerosols. For the average air parcel age of ~3 h, about 7% of NO<sub>y</sub> is removed from the atmosphere between emission and measurement, indicating that CO/NO<sub>x</sub> emissions ratios can be determined from NO<sub>y</sub> observations. See the Supplementary material for a more thorough discussion.

From the comparison between the observations and the modeled emissions, it is apparent that the NEI has the incorrect CO/NO<sub>x</sub> emissions ratio. To determine whether the NEI emissions of CO, NO<sub>x</sub>, or both are overestimated, observed concentrations of CO and NO<sub>y</sub> were compared with CMAQ model output.

### 3.3. Evaluation of CO emissions

To determine the NEI's accuracy of CO emissions, *in situ* CO observations were compared with the 1.33 km resolution CMAQ output. Fig. 1a shows observed CO concentrations for a representative flight day. Concentrations were relatively constant throughout the region, remaining between about 100 and 170 ppbv.

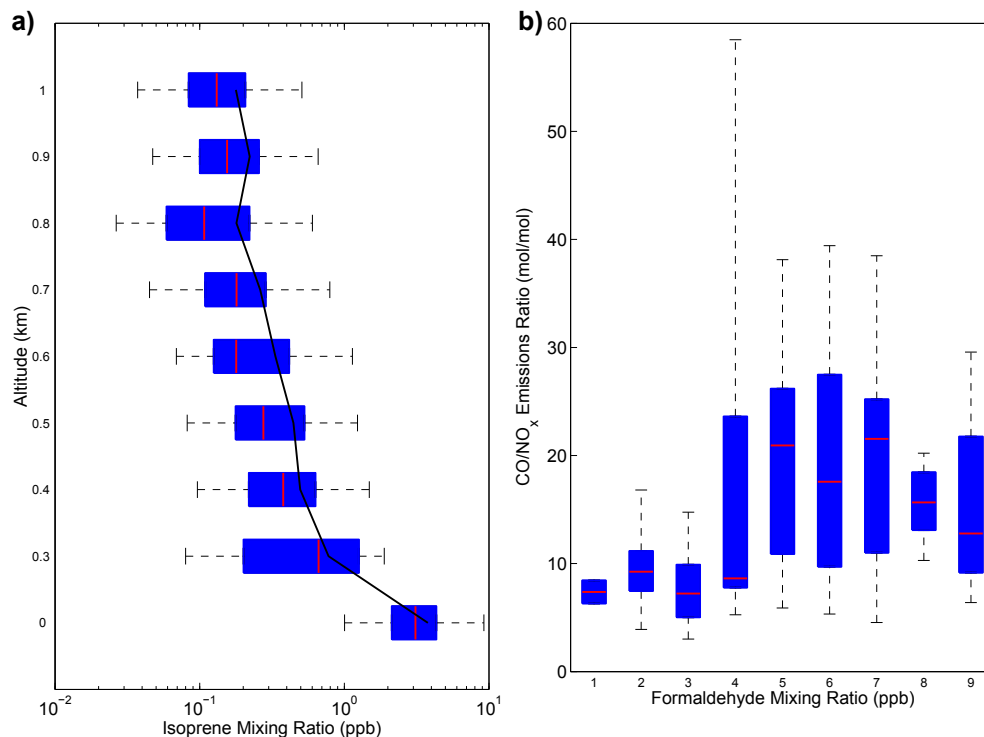


**Fig. 6.** a) Vertical isoprene profile over Essex, MD. Surface measurements are from MDE ground monitors. All other measurements were taken aboard the P3B. b) Comparison of CO/NO<sub>x</sub> emissions ratio to formaldehyde mixing ratio.

CMAQ output (Fig. 1b) has a similar spatial distribution with an overall high bias of 15 ppbv, indicating excellent agreement between model and observations.

All campaign observations are plotted against the CMAQ model output in Fig. 7a. As in Fig. 1, the model has a slight high bias, as most values rest above the 1:1 line. The mean observed CO concentration, for the entire campaign, was  $136 \pm 43$  ppbv ( $1\sigma$ ), with the model showing a high bias of 28 ppbv and a root mean square error (RMSE) of 48 ppbv. The relatively low bias suggests that mean CO emissions for the BWR are reasonable albeit a bit too high. The bias varied between +3% and +72% for the different flight days likely due to errors in boundary conditions and uncertainties in isoprene chemistry and emissions in CMAQ. The high bias was also consistent for all pressure levels, indicating that the model is, over this time period, capturing vertical mixing and not holding CO too close to the surface.

To evaluate both the CMAQ CO output and the NEI CO emissions, we used the MOPITT V5J product, which includes both the thermal and near infrared channels for improved sensitivity to near-surface CO, as compared to the thermal infrared only MOPITT product (Fig. 8a) (Deeter et al., 2012; Worden et al., 2010). The MOPITT V5 products and validation results are described in Deeter et al. (2013). CMAQ CO concentrations were averaged over the month of July 2011 in each grid cell, regridded to correspond with the MOPITT grid ( $1^\circ \times 1^\circ$ ), and values between 800 and 900 hPa were averaged to calculate a layer value, comparable to that of MOPITT. The model was then sampled using the MOPITT averaging kernel and *a priori* data. Results (Fig. 8b) show that the average CO concentration over the CMAQ domain was 123 ppbv, 4 ppbv lower than MOPITT, with an overall RMSE of 16.3 ppbv, showing excellent agreement between the model and satellite observations. CO concentrations over the urban portion of the BWR are slightly lower in CMAQ than in MOPITT, while CO is about 15% higher in CMAQ over the Delmarva Peninsula and Chesapeake Bay. These comparisons between CMAQ and MOPITT agree excellently with the *in situ* observations from the P3B.

Comparison of *in situ* and remote observations with CMAQ output indicates that the NEI is overestimating anthropogenic CO emissions. Combining the 21% high bias of the model with our estimate of the *in situ* CO production by isoprene, the NEI overpredicts CO concentrations by approximately 15%. This overprediction and the difference between observed and modeled CO/NO<sub>x</sub> emissions ratios indicate that the NEI must significantly overestimate NO<sub>x</sub> emissions.

#### 3.4. Evaluation of NO<sub>x</sub> emissions

Comparison of measured and modeled NO<sub>y</sub> mixing ratios (Fig. 7b) shows consistent and significant overestimation of NO<sub>y</sub> by CMAQ as well as weak correlation ( $r^2 = 0.29$ ). The observed mean NO<sub>y</sub> mixing ratio for the campaign was  $2.49 \pm 2.42$  ppbv ( $1\sigma$ ), a factor of two lower than the model ( $5.2 \pm 4.39$  ppbv). Table 2 shows the agreement for individual NO<sub>y</sub> constituents. NO, NO<sub>2</sub>, and HNO<sub>3</sub> all agree with observations within 25%, although there is a consistent high bias and low correlation. ΣPAN and ΣAN are overestimated by a factor of 2.3 and 3.0 respectively. The discrepancy between the measured and modeled NO<sub>y</sub> species in addition to SMOKE's incorrect emissions ratios indicate errors in both the model's NO<sub>y</sub> chemistry and the NEI's NO<sub>x</sub> emissions.

Model runs altering the chemistry and emissions confirm this statement. In addition to the previously discussed CMAQ run, two additional runs were conducted: one in which the alkyl nitrate reaction constant was increased by a factor of 10, bringing the lifetime in better agreement with observations in areas with high isoprene concentrations (Horowitz et al., 2007), and one combining this altered alkyl nitrate chemistry with a factor of two reduction in all mobile NO<sub>x</sub> emissions. A comparison of the NO<sub>y</sub> constituents from these runs is shown in Table 2. These model runs are meant to be illustrative of the relative impacts of chemistry and emissions and are not an attempt to model air quality precisely. Altering reaction kinetics brings modeled and measured ΣAN into better

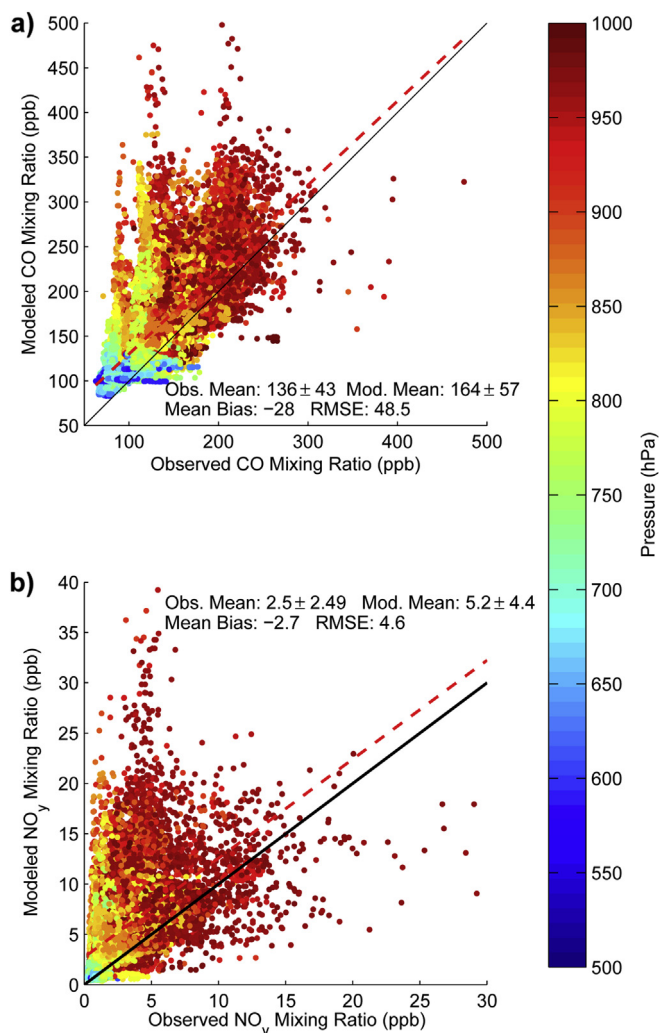


**Fig. 7.** a) Regression of measured and modeled CO for all flight days during DISCOVER-AQ. Values after means are  $1\sigma$ . b) Same as a) but for  $\text{NO}_y$ . Solid line is the 1:1 line; dashed line, the line of best fit.

agreement (last row, Table 2) but has little effect on the overall  $\text{NO}_y$  concentration, reducing the amount by only a fraction of a ppbv (Canty et al., in preparation). When the 50% reduction in mobile  $\text{NO}_x$  emissions is included, however, the modeled  $\text{NO}_y$  concentrations drop significantly, reducing the overall disagreement between measurement and model to 1.2. Measured and modeled  $\text{NO}$ ,  $\text{NO}_2$ , and  $\text{HNO}_3$  all agree within 20%, though  $\text{NO}$  and  $\text{NO}_2$  concentrations are both underestimated and there is still poor correlation for all three species ( $r^2 < 0.3$ ). Modeled  $\Sigma\text{PAN}$  is still a factor of 2.3 too high while  $\Sigma\text{AN}$  now agrees within 40%. Significant alterations to the model chemistry are still required.

Point source  $\text{NO}_x$  emissions (e.g. power plants and boilers) from SMOKE and from the Continuous Emissions Measurement System (CEMS) for the state of Maryland were compared for July 2011 to evaluate the accuracy of SMOKE's point source emissions, since the model was run before daily data were available. SMOKE emissions were approximately constant, while the monitored emissions showed significant temporal variability, varying by almost a factor of 5 (Fig. 9a). Although daily agreement between the model and CEMS is poor, the measured and modeled values agree within 1% on a monthly average. Modeled point source  $\text{NO}_x$  emissions cannot be responsible for the significant  $\text{NO}_y$  overestimation. This is further confirmed by Fig. 9b, which shows the ratio of CEMS to SMOKE  $\text{NO}_x$  emissions plotted against the ratio of observed to modeled  $\text{NO}_y$  mixing ratios. If daily discrepancies between measured and modeled point source emissions caused the modeled  $\text{NO}_y$  overestimation, days with CEMS measurements greater than SMOKE emissions ( $\text{CEMS}/\text{SMOKE} > 1$ ) would have a ratio of Measured/Modeled  $\text{NO}_y$  greater than 1. Fig. 9b shows no trend between the two ratios. Because the NEI estimates that 73% of Maryland's  $\text{NO}_x$  emissions stem from mobile sources and the point source emissions used in the CMAQ model runs are, on average, correct, emissions from the mobile sector are the most likely source of the overestimate of  $\text{NO}_x$  emissions.

#### 4. Discussion

$\text{CO}/\text{NO}_x$  emissions ratios in the BWR were found to be  $11.2 \pm 1.2$ , a factor of 1.21 higher than the NEI. Comparison between *in situ* observations, MOPITT, and CMAQ show that observed CO emissions are  $\sim 21 \pm 11\%$  higher than modeled emissions, with 4–7% of CO

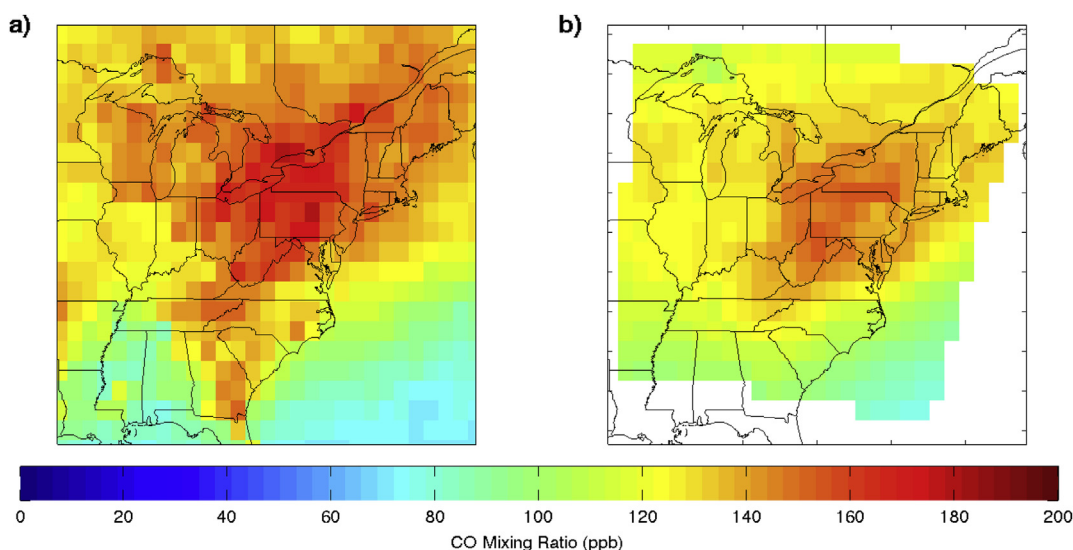


**Fig. 8.** a) MOPITT monthly averaged CO concentration at the 900 hPa level for July 2011 b) CMAQ monthly averaged CO concentration at the 900 hPa level with the MOPITT averaging kernel.

**Table 2**

Comparison between measured and modeled  $\text{NO}_y$  and its constituents for 3 model runs: a base case, a chemistry run (factor of 10 reduction in  $\Sigma\text{AN}$  lifetime), and a chemistry + emissions run ( $\Sigma\text{AN}$  lifetime and 50% mobile  $\text{NO}_x$  emissions reductions). Data are for the entire campaign. A positive bias indicates the model is higher than observations.

Species	Obs. mean	Base (ppbv)		Chemistry (ppbv)		Chem + emissions (ppbv)	
		Model mean	Model bias	Model mean	Model bias	Model mean	Model bias
$\text{NO}_y$	2.5	5.2	2.7	4.5	2.1	3.7	1.2
$\text{HNO}_3$	1.07	1.3	0.26	1.5	0.39	1.1	0.03
$\text{NO}$	0.17	0.20	0.022	0.19	0.017	0.14	-0.03
$\text{NO}_2$	0.78	0.85	0.068	0.87	0.093	0.64	-0.14
PAN	0.61	1.4	0.81	1.6	0.97	1.4	0.77
Alkyl Nitrates	0.32	0.96	0.65	0.48	0.16	0.44	0.12

concentration stemming from isoprene oxidation. The NEI overestimates CO emissions by  $15 \pm 11\%$  ( $1\sigma$ ).

Fig. 10 shows the ratio of the observed  $\text{CO}/\text{NO}_x$  emissions ratio to that predicted by the NEI for each location corrected for *in situ* CO production and errors in the NEI's CO emissions. Values greater than 1 indicate a higher ratio than that predicted by the NEI. Because the data

are corrected for CO, the resulting values are also the ratio of observed to NEI predicted  $\text{NO}_x$  emissions, showing explicitly the NEI's overestimation of  $\text{NO}_x$  emissions across the experimental domain. Combining these data with the uncertainties in dry deposition and aerosolization of  $\text{NO}_y$  species yields an overestimation of  $\text{NO}_x$  emissions by the NEI of  $44 \pm 26\%$  ( $1\sigma$ ). Using a linear, least squares method with CO as the independent variable, instead of the orthogonal regression previously discussed, yields an overestimate in  $\text{NO}_x$  emissions of  $75 \pm 24\%$ . Because uncertainty in the CO measurement is an order of magnitude lower than for  $\text{NO}_y$ , this regression method is equally valid, implying that the true NEI  $\text{NO}_x$  emissions overestimate is likely in the region of overlap between the two, or 51–70%.

Comparison of modeled and measured point source  $\text{NO}_x$  emissions shows excellent agreement, implying that the most likely source of error in the NEI  $\text{NO}_x$  emissions is mobile sources, which make up approximately 50–75% of  $\text{NO}_x$  emissions in the BWR depending on the time of day. Assumptions in MOVES2010 may be responsible for this  $\text{NO}_x$  emissions overestimate. Further exploration into the model mechanics is needed for definitive determination of the overestimate source(s). The model's treatment of emissions from aging vehicles is one likely contributor; the NEI overestimate of  $\text{NO}_x$  emissions could indicate that engines produce less  $\text{NO}_x$  and catalytic converters degrade more slowly than

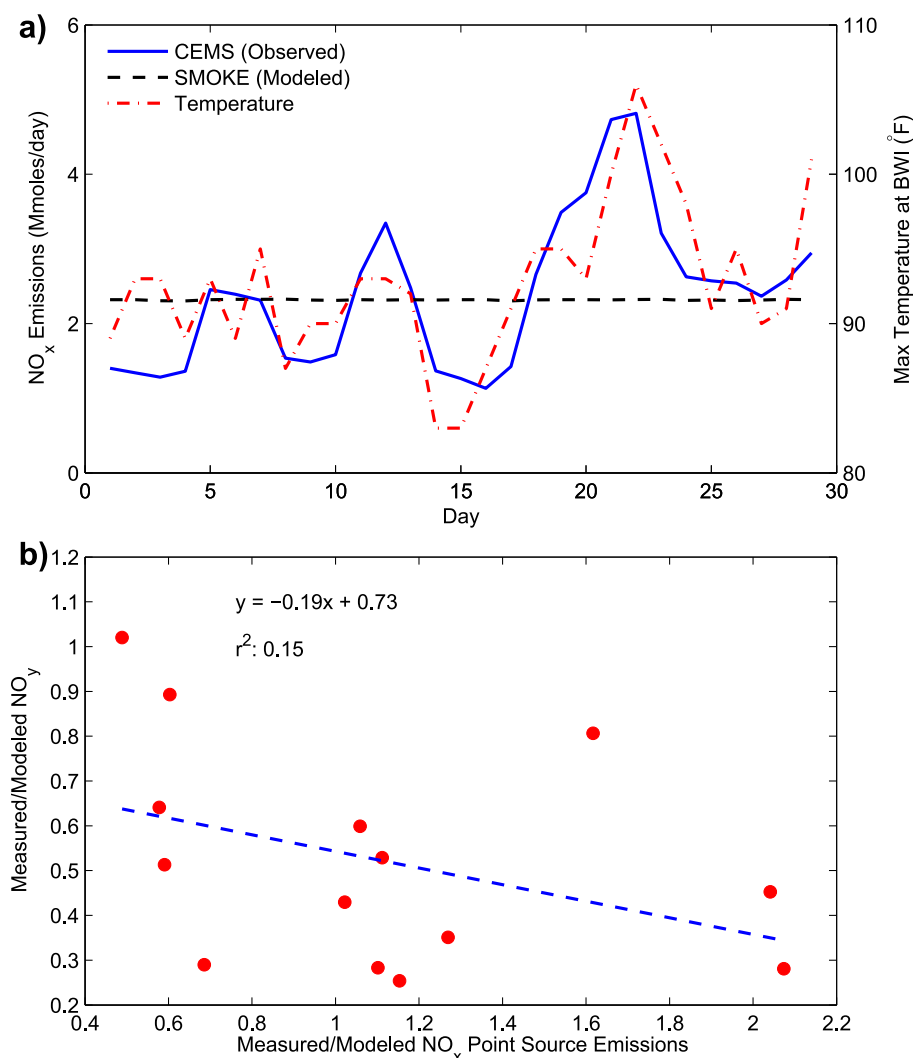


**Fig. 9.** a) Comparison of point source emissions from SMOKE and from observations (CEMS). The maximum daily temperature at Baltimore Washington International Airport is provided for reference. b) Ratio of the average observed and modeled  $\text{NO}_y$  concentrations versus the ratio of measured point source  $\text{NO}_x$  emissions to modeled emissions.



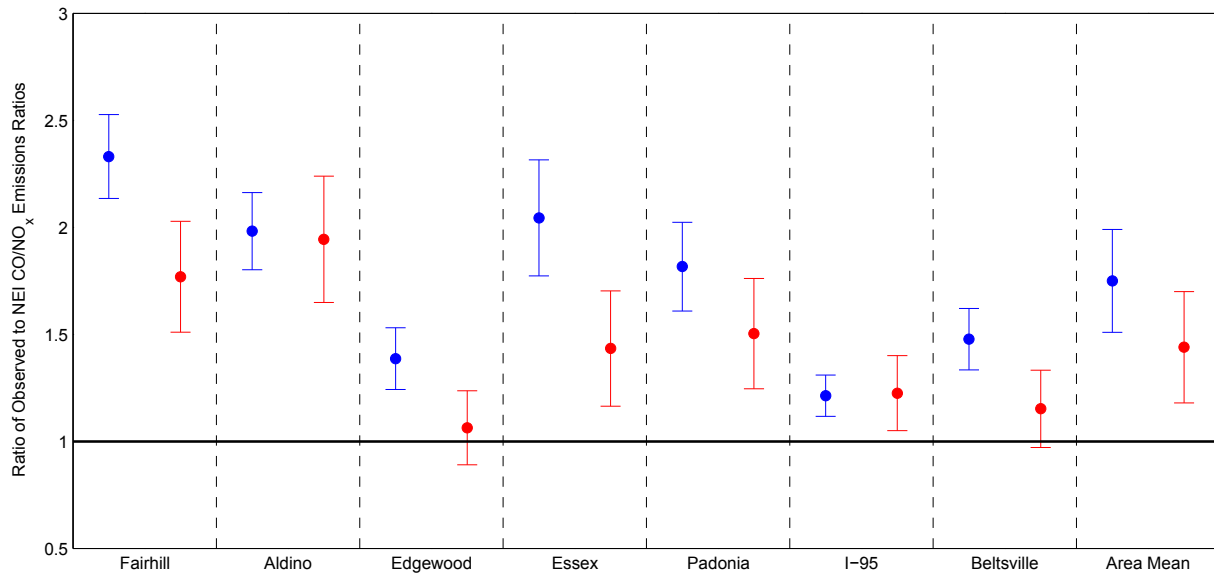


**Fig. 10.** Ratio of observed CO/NO<sub>x</sub> emissions ratios to those predicted by the NEI by location. Values are corrected for CO uncertainties. Blue are derived using the linear least squares method, and red are derived with an orthogonal linear regression. Uncertainties are the 1 $\sigma$  uncertainties in the NEI values and observations added in quadrature. (For interpretation of the references to color in this figure legend, the reader is referred to the web version of this article.)

assumed by MOVES2010. MOVES2010 likely fails to capture dependence of NO<sub>x</sub> emissions on vehicle age accurately. Similarly, Bishop et al. (2012) shows that 1% of the vehicle fleet could emit as much as 15% of total NO<sub>x</sub> emissions, indicating that misrepresentation of the attributes of these outliers in emissions inventories could have significant effects on the estimated emissions. Incorrect emissions apportionment to the diesel portions of the on- and off-road fleets would lead to significant errors in the ratio of CO to NO<sub>x</sub> emissions. Incorrect emission factors are also another possible source of error. Lindhjem et al. (2012) found that the use of MOVES2010 emissions factors increased NO<sub>x</sub> emissions by 50% in comparison to those found in the previous EPA model, MOBILE6. While further studies with the recently released 2011 NEI are needed, its CO/NO<sub>x</sub> ratio for Maryland is even lower than the values used in this study.

If mobile emissions are indeed overestimated by 51–70%, then the relative importance of NO<sub>x</sub> emissions from other sectors, particularly point and area sources, increases dramatically. It will then be even more pressing to ensure the development of effective policies to reduce NO<sub>x</sub> emissions from these other sources to decrease ambient NO<sub>y</sub> concentrations, reduce O<sub>3</sub> production, and improve air quality. Because models indicate that, for the majority of the O<sub>3</sub> non-attainment area, that areas of NO<sub>x</sub> inhibiting O<sub>3</sub> formation are very small and Maryland is in the NO<sub>x</sub> limited regime for O<sub>3</sub> production (Chameides et al., 1992), significant reductions in NO<sub>x</sub> emissions should result in significant and observable reductions in O<sub>3</sub> mixing ratios and a dramatic improvement in air quality. Reductions in NO<sub>x</sub> may be more effective than predicted by CMAQ, but policy measures aiming to reduce NO<sub>x</sub> emissions must be directed at the correct sectors.

## Acknowledgments

We thank Andreas Beyersdorf and Bruce Anderson (NASA Langley) for aerosol data, Ron Cohen (UC Berkeley) for TDLIF measurements, and David Krask (MDE) for surface isoprene observations. This work was supported by grants from NASA and AQAAT.

## Appendix A. Supplementary data

Supplementary data related to this article can be found at <http://dx.doi.org/10.1016/j.atmosenv.2014.07.004>.

## References

- Ban-Weiss, G., et al., 2008. Long-term changes in emissions of nitrogen oxides and particulate matter from on-road gasoline and diesel vehicles. *Atmos. Environ.* 42 (2), 220–232. <http://dx.doi.org/10.1016/j.atmosenv.2007.09.049>.
- Bell, M., Peng, R., Dominici, F., 2006. The exposure-response curve for ozone and risk of mortality and the adequacy of current ozone regulations. *Environ. Health Perspect.* 114 (4), 532–536.
- Bishop, G., Schuchmann, B., Stedman, D., Lawson, D., 2012. Multispecies remote sensing measurements of vehicle emissions on Sherman Way in Van Nuys, California. *J. Air Waste Manag. Assoc.* 62 (10), 1127–1133. <http://dx.doi.org/10.1080/10962247.2012.699015>.
- Brioude, J., et al., 2013. Top-down estimate of surface flux in the Los Angeles Basin using a mesoscale inverse modeling technique: assessing anthropogenic emissions of CO, NO<sub>x</sub> and CO<sub>2</sub> and their impacts. *Atmos. Chem. Phys.* 13 (7), 3661–3677. <http://dx.doi.org/10.5194/acp-13-3661-2013>.
- Canty, T., et al., 2014. Ozone and NO<sub>x</sub> Chemistry in the Eastern US: Evaluation of CMAQ/CB05 with OMI Data (in preparation).
- Castellanos, P., et al., 2011. Ozone, oxides of nitrogen, and carbon monoxide during pollution events over the eastern United States: an evaluation of emissions and vertical mixing. *J. Geophys. Res.* 116 (D16) <http://dx.doi.org/10.1029/2010jd014540>.
- Chameides, W., et al., 1992. Ozone precursor relationships in the ambient atmosphere. *J. Geophys. Res. Atmos.* 97 (D5), 6037–6055.
- Cooper, O., Gao, R.-S., Tarasick, D., Leblanc, T., Sweeney, C., 2012. Long-term ozone trends at rural ozone monitoring sites across the United States, 1990–2010. *J. Geophys. Res. Atmos.* 117 (D22) <http://dx.doi.org/10.1029/2012jd018261> n/a–n/a.
- Crutzen, P., Heidt, L., Krasnec, J., Pollock, W., Seiler, W., 1979. Biomass burning as a source of atmospheric gases: CO, H<sub>2</sub>, N<sub>2</sub>O, NO, CH<sub>3</sub>Cl, and COS. *Nature* 282 (5736), 253–256. <http://dx.doi.org/10.1038/282253a0>.
- Dallmann, T., Harley, R., 2010. Evaluation of mobile source emission trends in the United States. *J. Geophys. Res. Atmos.* 115 <http://dx.doi.org/10.1029/2010jd013862>.
- Deeter, M., et al., 2013. Validation of MOPITT Version 5 thermal-infrared, near-infrared, and multispectral carbon monoxide profile retrievals for 2000–2011. *J. Geophys. Res. Atmos.* 118 (12), 6710–6725. <http://dx.doi.org/10.1002/jgrd.50272>.
- Deeter, M., Worden, H., Edwards, D., Gille, J., Andrews, A., 2012. Evaluation of MOPITT retrievals of lower-tropospheric carbon monoxide over the United States. *J. Geophys. Res. Atmos.* 117 <http://dx.doi.org/10.1029/2012jd017553>.
- Farmer, D., Wooldridge, P., Cohen, R., 2006. Application of thermal-dissociation laser induced fluorescence (TD-LIF) to measurement of HNO<sub>3</sub>, Sigma alkyl

- nitrate, Sigma peroxy nitrates, and NO<sub>2</sub> fluxes using eddy covariance. *Atmos. Chem. Phys.* 6, 3471–3486.
- Fiore, A., Jacob, D., Logan, J., Yin, J., 1998. Long-term trends in ground level ozone over the contiguous United States, 1980–1995. *J. Geophys. Res. Atmos.* 103 (D1), 1471–1480. <http://dx.doi.org/10.1029/97jd03036>.
- Fujita, E., et al., 2012. Comparison of the MOVES2010a, MOBILE6.2, and EMFAC2007 mobile source emission models with on-road traffic tunnel and remote sensing measurements. *J. Air Waste Manag. Assoc.* 62 (10), 1134–1149. <http://dx.doi.org/10.1080/10962247.2012.699016>.
- Goldberg, D., et al., 2014. Higher surface ozone concentrations over the Chesapeake Bay than over the adjacent land: observations and models from the DISCOVER-AQ and CBODAQ campaigns. *Atmos. Environ.* 84, 9–19. <http://dx.doi.org/10.1016/j.atmosenv.2013.11.008>.
- He, H., et al., 2013. Trends in emissions and concentrations of air pollutants in the lower troposphere in the Baltimore/Washington airshed from 1997 to 2011. *Atmos. Chem. Phys. Discuss.* 13 (2), 3135–3178. <http://dx.doi.org/10.5194/acpd-13-3135-2013>.
- Horowitz, L., et al., 2007. Observational constraints on the chemistry of isoprene nitrates over the eastern United States. *J. Geophys. Res. Atmos.* 112 (D12) <http://dx.doi.org/10.1029/2006jd007747>.
- Hudman, R., et al., 2008. Biogenic versus anthropogenic sources of CO in the United States. *Geophys. Res. Lett.* 35 (4), 5. <http://dx.doi.org/10.1029/2007gl032393>.
- Lancaster, D., et al., 2000. Difference-frequency-based tunable absorption spectrometer for detection of atmospheric formaldehyde. *Appl. Opt.* 39 (24), 4436–4443. <http://dx.doi.org/10.1364/ao.39.004436>.
- Lindhjem, C., Pollack, A., DenBleyker, A., Shaw, S., 2012. Effects of improved spatial and temporal modeling of on-road vehicle emissions. *J. Air Waste Manag. Assoc.* 62 (4), 471–484. <http://dx.doi.org/10.1080/10962247.2012.658955>.
- Lindinger, W., Hansel, A., Jordan, A., 1998. Proton-transfer-reaction mass spectrometry (PTR-MS): on-line monitoring of volatile organic compounds at pptv levels. *Chem. Soc. Rev.* 27 (5), 347–354. <http://dx.doi.org/10.1039/a827347z>.
- Loughner, C., et al., 2014. Impact of bay breeze circulations on surface air quality and boundary layer export. *J. Appl. Meteorol. Climatol.* <http://dx.doi.org/10.1175/JAMC-D-13-0323.1>.
- Maryland Department of Transportation, <http://www.roads.maryland.gov/index.aspx?PageId=251>.
- McDonald, B., Dallmann, T., Martin, E., Harley, R., 2012. Long-term trends in nitrogen oxide emissions from motor vehicles at national, state, and air basin scales. *J. Geophys. Res. Atmos.* 117 (D21) <http://dx.doi.org/10.1029/2012jd018304> n/a–n/a.
- Morales, R., 1998. Carbon Monoxide, Ozone, and Hydrocarbons in the Baltimore Metropolitan Area. University of Maryland, College Park.
- Parrish, D., 2006. Critical evaluation of US on-road vehicle emission inventories. *Atmos. Environ.* 40 (13), 2288–2300. <http://dx.doi.org/10.1016/j.atmosenv.2005.11.033>.
- Pollack, I., et al., 2013. Trends in ozone, its precursors, and related secondary oxidation products in Los Angeles, California: a synthesis of measurements from 1960 to 2010. *J. Geophys. Res. Atmos.* 118 (11), 5893–5911. <http://dx.doi.org/10.1002/jgrd.50472>.
- Ridley, B., Grahek, F., 1990. A small, low-flow, high-sensitivity reaction vessel for NO chemiluminescence detectors. *J. Atmos. Ocean. Technol.* 7 (2), 307–311. [http://dx.doi.org/10.1175/1520-0426\(1990\)007<0307:aslfs>2.0.co;2](http://dx.doi.org/10.1175/1520-0426(1990)007<0307:aslfs>2.0.co;2).
- Sachse, G., Hill, G., Wade, L., Perry, M., 1987. Fast-response, high-precision carbon monoxide sensor using a tunable diode laser absorption technique. *J. Geophys. Res. Atmos.* 92 (D2), 2071–2081. <http://dx.doi.org/10.1029/JD092iD02p02071>.
- Seinfeld, J., Pandis, S., 2006. *Atmospheric Chemistry and Physics: From Air Pollution to Climate Change*, second ed. John Wiley & Sons, Hoboken, NJ, p. 1203.
- US EPA, 2008. *Integrated Science Assessment for Oxides of Nitrogen – Health Criteria*. EPA/600/R-08/071 Rep., US EPA, Washington, DC.
- US EPA, 2010. *Integrated Science Assessment for Carbon Monoxide*. EPA/600/R-09/019F Rep., United States Environmental Protection Agency, Washington, DC.
- US EPA, 2011. *Emissions Inventory Final Rule TSD*. EPA-HQ-OAR-2009-0491 Rep., U.S. Environmental Protection Agency Office of Air and Radiation, Office of Air Quality Planning and Standards, Air Quality Assessment Division, Washington, DC.
- US EPA, 2012. *User Guide for MOVES2010b*. EPA-420-B-12-001b Rep., 202 pp. Office of Transportation and Air Quality, US Environmental Protection Agency, Washington, DC.
- Williams, E., et al., 2009. Emissions of NO<sub>x</sub>, SO<sub>2</sub>, CO, and HCHO from commercial marine shipping during Texas Air Quality Study (TexAQS) 2006. *J. Geophys. Res. Atmos.* 114 <http://dx.doi.org/10.1029/2009jd012094>.
- Worden, H., et al., 2010. Observations of near-surface carbon monoxide from space using MOPITT multispectral retrievals. *J. Geophys. Res. Atmos.* 115 <http://dx.doi.org/10.1029/2010jd014242>.
- Yu, S., et al., 2012. Comparative evaluation of the impact of WRF-NMM and WRF-ARW meteorology on CMAQ simulations for O<sub>3</sub> and related species during the 2006 TexAQS/GoMACCS campaign. *Atmos. Pollut. Res.* <http://dx.doi.org/10.5094/apr.2012.015>.